NATIONAL AERONAUTICS AND SPACE ADMINISTRATION

Technical Report 32-1341

Landing Dynamics Program for Axisymmetric Impact Attenuating Vehicles (LANDIT)

Albert C. Knoell

JET PROPULSION LABORATORY
CALIFORNIA INSTITUTE OF TECHNOLOGY
PASADENA, CALIFORNIA
November 15, 1968

NATIONAL AERONAUTICS AND SPACE ADMINISTRATION

Technical Report 32-1341

Landing Dynamics Program for Axisymmetric Impact Attenuating Vehicles (LANDIT)

Albert C. Knoell

JET PROPULSION LABORATORY
CALIFORNIA INSTITUTE OF TECHNOLOGY
PASADENA, CALIFORNIA
November 15, 1968

TECHNICAL REPORT 32-1341

Prepared Under Contract No. NAS 7-100
National Aeronautics & Space Administration

Preface

The work described in this report was performed by the Engineering Mechanics Division of the Jet Propulsion Laboratory.

Acknowledgment

Grateful acknowledgment is made to Mr. Robert Patton of the Systems Division, Jet Propulsion Laboratory, in programming LANDIT and Mr. Michael Gaitens of the Spacecraft Department, General Electric Company, in developing and coding the footprint geometry analysis subroutine.

Contents

Contents (contd)

Figures

Abstract

A computer program (LANDIT) is described that predicts the dynamic landing response characteristics of axisymmetric impact attenuating vehicles consisting of a rigid payload and a crushable impact limiter system. The program is based on the solution of a planar landing dynamics problem considering vehicle impacts against plane unyielding surfaces. Initial conditions that must be provided include impact velocity vector, touchdown angle, vehicle pitch rate, surface slope, and coefficient of friction.

Landing Dynamics Program for Axisymmetric Impact Attenuating Vehicles (LANDIT)

I. Introduction

A digital computer program has been developed at the Jet Propulsion Laboratory to predict the dynamic landing response characteristics of axisymmetric impact attenuating vehicles that consist of a rigid payload and a crushable impact limiter system. This program (acronym: LANDIT) is intended for use primarily as a design tool in the structural design of lunar or planetary hard-landing vehicles. In use, the program generates response data for vehicle impacts against plane unyielding surfaces. Since input preparation for the program is simple, engineering personnel who have had only slight training in computer programming can fully utilize the capabilities of LANDIT. This program has been written for the IBM 7090/94 computer for execution under the IBFTC monitor system.

In general, input to the program must be provided in three basic categories:

(1) Vehicle description, consisting of geometry and material property data.

(2) Vehicle initial touchdown conditions.

(3) Impact surface characteristics.

Given the proper input, LANDIT will perform computations to provide the user as output a complete set of vehicle CG displacement, velocity, and acceleration-time histories of the impact event. In addition, the program provides the user continuous data regarding the magnitude of the crushing force and the amount of mechanical energy dissipated. During the impact event, LANDIT will also monitor and print out acceleration-time data for payload points other than vehicle gravity center, as specified by the user.

The program is based on the solution of a planar landing dynamics problem. The vehicle degrees-of-freedom consist of the horizontal and vertical displacements of the gravity center relative to the impact surface and the rotation of the vehicle about the center of gravity in the plane of the admissible displacements. The solution is developed by numerically solving a set of three nonlinear differential equations of motion. In the solution process, the program utilizes two major subroutines: an integration subroutine[1] and a footprint geometry analysis subroutine

[1]Private communication, Dr. F. T. Krogh.

(Ref. 1). An automatic error control is contained in the integration subroutine to define convergence of the solution to the system of equations.

The program has been used to predict the impact response of a previously designed disc-type Mars prototype landing vehicle (Ref. 2). Correlation of the predicted response data with development test results is good.

Machine running time on the 7094 depends largely on the vehicle geometry description. As a general trend, the running time varies from approximately 1 to 10 min for elementary to rather complex vehicle geometries.

The time required to generate input for the program again largely depends on the vehicle geometry. Use of a vehicle layout drawing, from which dimensions and angles can be scaled, facilitates the input-generating process considerably. Input for the Mars landing vehicle (Ref. 2) was generated in approximately one hour.

II. Program Description

A. Vehicle Idealization

1. Payload and limiter elements. The structural configuration of any axisymmetric impact attenuating vehicle can be idealized as a set of payload and limiter annular elements developed by rotating the element cross section about the vehicle z axis. Consider now the y-z section of a general lander vehicle (Fig. 1). From the symmetry restriction, it is clear that only the $+y$ half-plane of the vehicle cross section need be considered to define the overall structural geometry. As indicated in Fig. 1, the cross section of any element is at most a polygon. (No curved boundaries are permitted in the idealization of the vehicle cross section.) A payload element cross section is always triangular, whereas a limiter element cross section may be triangular or quadrilateral.

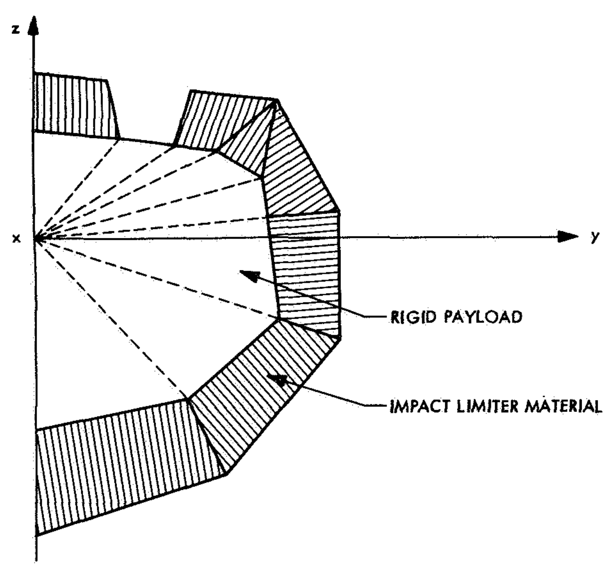

Fig. 1. General landing vehicle cross section

The vehicle overall structural geometry is completely defined once all limiter element cross sections are described. It should be noted that the only limiter cross section that is geometrically acceptable to the program is a quadrilateral. A quadrilateral (Fig. 2a) is defined to the program by giving the y, z coordinates of the four corner points. The corner points must be numbered 1 through 4 moving in a consecutive clockwise manner around the perimeter.

In idealizing a limiter element cross section, the following restrictions apply:

(1) The element side, described by the points numbered 1 and 4, (side 1-4) is always coincident with the payload-limiter interface.

(2) No element side may have zero length. (The sole exception to this restriction is discussed below.)

(3) Opposite sides of a quadrilateral may not cross, i.e., side 1-4 does not intersect 2-3, and side 1-2 does not intersect side 3-4.

Although the program will accept only quadrilateral elements which meet the above restrictions, it is possible to simulate a limiter triangular element without violating the above rules. This is done by making sides 1-2 and 2-3 colinear or alternately by making sides 2-3 and 3-4 colinear. See Fig. 2b as an example.

Since there may be annular areas of the payload not covered by impact limiter material (Fig. 1), the program has the capability to handle zero-thickness limiter elements. These elements are input with identical coordinates for points 1 and 2 and for 3 and 4, respectively (Fig. 2c). Note that the length of side 1-4 equals that of side 2-3 and that this length must be greater than zero. The use of zero-thickness elements to complete the vehicle description is recommended, although not mandatory.

The program numbers the limiter elements consecutively as they are read. If the structure is symmetric with respect to the x-y plane, only data for one quadrant need be given. The program will then proceed to build the

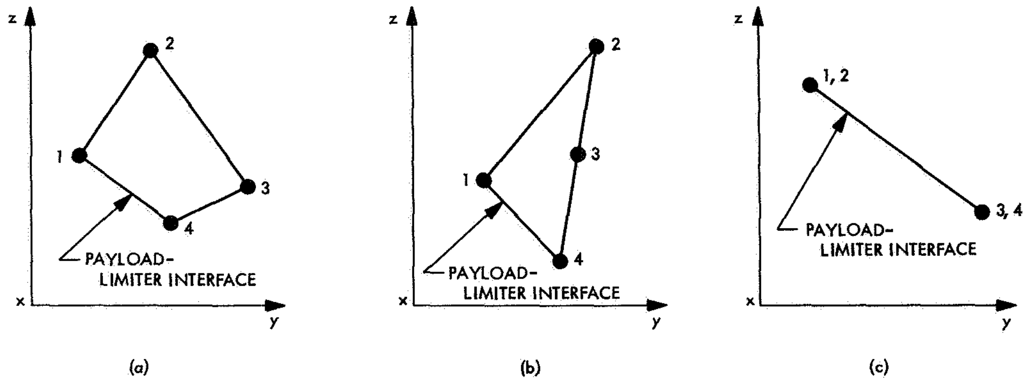

Fig. 2. Possible limiter element configurations: (a) quadrilateral, (b) triangular, (c) linear

elements in the other quadrant by reversing the signs of the given z coordinates. Element numbers for the generated quadrant are the negative of those assigned to the elements which were input directly.

2. *Limiter pads.* Any of the limiter annular elements may be divided into a series of pads in the x-y plane as shown in Fig. 3. This program capability was provided to enable the user to better idealize an actual landing vehicle which is usually fabricated in this manner. The pads are formed by constructing half-planes which contain the z axis. In the section shown in Fig. 3, this construction results in sectors of concentric circles. The traces of the half-planes which separate the pads represent the limiter glue lines developed during element fabrication. In general, the pad geometry is restricted such that all pads of a given element are identically the same. The program numbers the pads consecutively in the direction of a positive rotation about the z axis. Pad number one either contains the $+y$ axis or abuts it and lies in the $+x$, $+y$ quadrant.

3. *Limiter pad fiber orientation.* As may be inferred from Figs. 1 and 3, the fiber orientation within each limiter pad is considered constant. Thus the definition of the orientation of a single pad fiber automatically defines the orientation of all fibers in the pad. This idealization is consistent with the actual fiber orientation in any pad of energy-dissipating material. It should be noted that the orientation defined for a given pad fiber with respect to the z axis is considered the same for all pads of the respective limiter element.

B. Coordinate Systems

As shown in Fig. 4, three coordinate systems are used to describe the impact position of a landing vehicle in space. All three systems are right-handed and consist of three orthogonal axes with mutually parallel "X" axes. The ground coordinate system ($\overline{X}$, $\overline{Y}$, $\overline{Z}$) is oriented such that the $\overline{Z}$ axis is aligned with the gravity vector, positive upward, and the $\overline{Y}$ axis is in the direction of the maximum

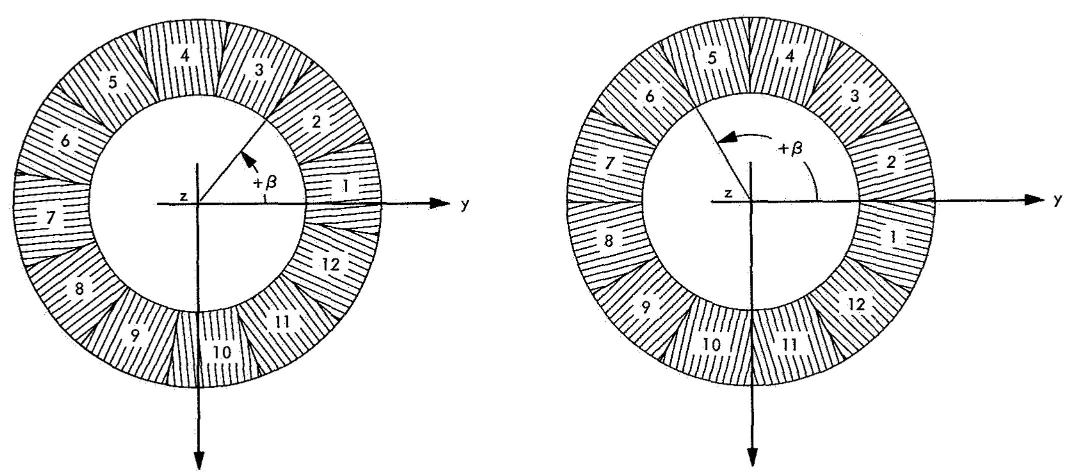

Fig. 3. Typical x-y section showing limiter pads and number sequence

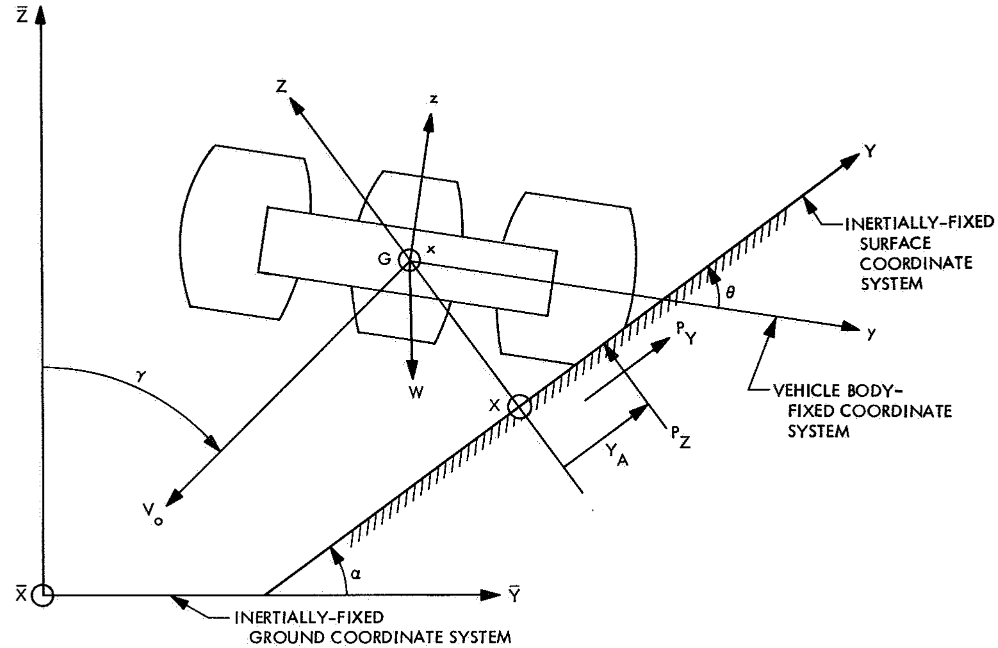

Fig. 4. LANDIT coordinate systems

surface slope. This system is inertially fixed and serves to define the surface slope angle α, and the impact velocity angle γ.

The surface coordinate system (X, Y, Z) differs from the ground coordinate system only by the rotation α about the $\bar{X}$ axis. In surface coordinates, the X and Y axes lie in the plane of the surface and the Z axis is normal to the surface, positive upward. At time $t = 0$, the origin of this inertially-fixed system is taken such that the Z axis passes through the vehicle gravity center, thereby eliminating an initial lateral displacement input.

The vehicle body-fixed coordinate system (x,y,z) has its origin at the center of gravity and moves with the vehicle. The z axis is positive upward along the vehicle centerline and the y axis is positive in the direction of the maximum surface slope. The vehicle coordinate system differs from the surface coordinate system by a rotation θ about the X axis.

C. Equations of Motion for Vehicle Gravity Center

Considering dynamic force equilibrium in the surface coordinate system (Fig. 4), the following set of differential equations can be developed:

$$\ddot{Z}_G = g\left(\frac{P_Z}{W} - \cos\alpha\right) \tag{1}$$

$$\ddot{Y}_G = g\left(\frac{P_Y}{W} - \sin\alpha\right) \tag{2}$$

$$\ddot{\theta} = \frac{1}{I}\left(P_Z Y_A + P_Y Z_G\right) \tag{3}$$

Where

$\ddot{Z}_G$ = acceleration of vehicle CG in Z direction

$\ddot{Y}_G$ = acceleration of vehicle CG in Y direction

$\ddot{\theta}$ = acceleration of vehicle about CG

g = acceleration due to gravity

α = principal surface slope

I = total vehicle mass moment of inertia about actual vehicle CG

P_Z = total instantaneous crushing force in Z direction

Y_A = moment arm of crushing force

P_Y = total instantaneous friction force in Y direction

Z_G = displacement of vehicle CG in Z direction

W = total vehicle weight

These three equations simultaneously govern the motion of the vehicle gravity center during the impact event. The independent variables in this set of equations are the two displacements, Y_G and Z_G, and the rotation θ. A numerical solution for this set of equations can be generated, provided the crushing force, P_Z, and the friction force, P_Y, are developed in terms of these variables.

From Fig. 4 it is evident that the crushing force is a function of the two variables, Z_G and θ. In addition, the magnitude of the crushing force depends on the limiter material properties and vehicle geometry. Details relating to the analytic development of the limiter crushing force are presented in the following section.

Since the friction force is directly related to the crushing force through the coefficient of sliding friction, no consideration need be given to the development of the friction force in terms of the independent variables. The magnitude of the friction force can be determined from the expression:

$$|P_Y| = |\mu_0 P_Z| \tag{4}$$

where μ_0 = coefficient of sliding friction.

The direction of application of the friction force, however, depends on the local motion of the vehicle at the limiter–surface interface. To describe this motion, it is clear that:

$$\dot{Y}_c = \dot{Y}_G + \dot{\theta} Z_G \tag{5}$$

where

$\dot{Y}_c$ = vehicle velocity at the limiter–surface interface

$\dot{Y}_G$ = velocity of vehicle CG in Y direction

$\dot{\theta}$ = angular velocity of the vehicle about CG

Knowing $\dot{Y}_c$, the magnitude and direction of P_Y can readily be combined into the following set of relations:

$$\begin{aligned} &\text{If } \dot{Y}_c > 0 && P_Y = -\mu_0 P_Z \\ &\text{If } \dot{Y}_c < 0 && P_Y = \mu_0 P_Z \\ &\text{If } \dot{Y}_c = 0 && P_Y = 0 \end{aligned} \tag{6}$$

Greater computational stability is provided, however, by eliminating the abrupt change in friction force direction of application that exists at $Y_c = 0$. Considering the friction force to be equal to the product of a variable coefficient of sliding friction and the crushing force, a graphic illustration of the change in force direction, as given by Eq. (6), is shown in Fig. 5a.

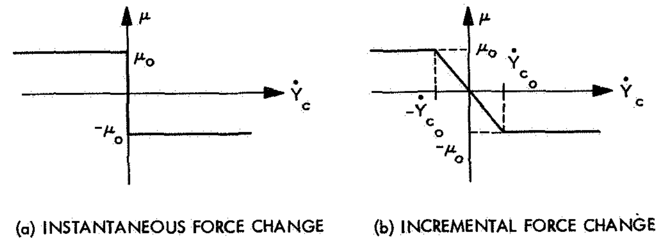

Fig. 5. Coefficient of sliding friction vs vehicle velocity at limiter-surface interface

However, on the basis of the *Surveyor* project development experience (Ref. 3) it has been found that a variation in coefficient of sliding friction, as indicated in Fig. 5b, is more appropriate. Incorporating this change in friction force direction into the final determination of the friction force results in the following set of relations:

$$\begin{aligned} &\text{If } \dot{Y}_c \geq \dot{Y}_{c_0}, && P_Y = -\mu_0 P_Z \\ &\text{If } \dot{Y}_c \leq -\dot{Y}_{c_0}, && P_Y = \mu_0 P_Z \\ &\text{If } -\dot{Y}_{c_0} < \dot{Y}_c < \dot{Y}_{c_0}, && P_Y = -\mu_0 \left(\frac{\dot{Y}_c}{\dot{Y}_{c_0}}\right) P_Z \end{aligned} \tag{7}$$

Consistent with Ref. 3, a value of $\dot{Y}_{c_0} = 0.05$ fps has been built into the program.

D. Limiter Crushing Force

The limiter crushing force, P_Z, is computed from the relation:

$$P_Z = \sum_{i=1}^{M} \sum_{n=1}^{N} \sigma_{in} \, a_{in} \tag{8}$$

where

σ_{in} = limiter crushing stress of the n^{th} pad of the i^{th} element

a_{in} = area at the crushing surface of the n^{th} pad of the i^{th} element

M = total number of limiter elements in vehicle description

N = total number of pads in a limiter element

The area at the crushing surface rather than at the limiter crushing boundary (e.g., see Refs. 4 and 5) was used primarily since no accurate measure of the thickness efficiency effect (defined in the limit as the ratio of the maximum usable stroke to the total available stroke) on the response of a general limiter pad during crushing can be developed. Neglecting the effect of thickness efficiency on an individual pad basis should not significantly affect the program results. The effect of thickness efficiency on the total degree of limiter crushability can be approximated, however, by idealizing a slightly oversized payload. By so doing, a final "bottomed-out" position of the limiter material can be established for the particular vehicle configuration under study.

The pad area at the crushing surface is developed using the footprint analysis subroutine program referred to previously. Very briefly, this subroutine determines each pad crushing area and the first moment of that area about the x axis for any combination of Z_G and θ. Knowing the first moment of a pad area and the crushing stress acting on that pad, the total moment arm, Y_A, used in Eq. (3) can then be computed from the relation:

$$Y_A = \frac{\sum_{i=1}^{M} \sum_{n=1}^{N} \sigma_{in}\, a_{in}\, l_{in}}{P_Z} \tag{9}$$

where l_{in} = moment arm of n^{th} pad of the i^{th} element about x axis. As a matter of convenience, all pad area and moment computations are made in the vehicle coordinate system.

In determining the pad crushing stress, σ_{in}, consideration must be given to the reduction in axial crushing stress due to off-axis loading. Accordingly, the general expression for σ_{in} may be written as:

$$\sigma_{in} = \sigma_0\, k_{(\psi_{in})} \tag{10}$$

where

σ_0 = axial crushing stress of limiter material

k = nondimensional crushing stress reduction parameter

ψ_{in} = angle of loading of n^{th} pad of the i^{th} limiter element

For most limiter energy-dissipating materials the off-axis load reduction parameter has been experimentally established (Refs. 6 and 7). The relationship used in this program is based on Fig. 6 and may be quantitatively

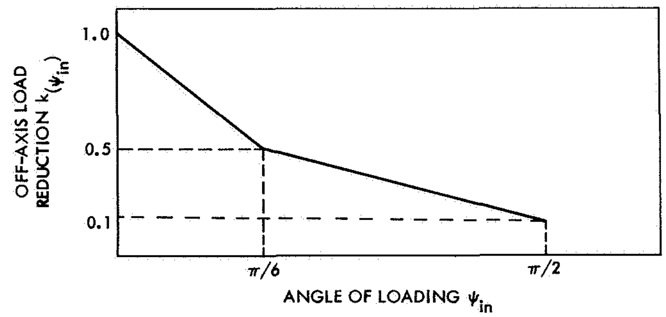

Fig. 6. Off-axis load reduction parameter vs angle of loading

written as:

$$k_{(\psi_{in})} = -\frac{3}{\pi}\psi_{in} + 1 \cdots 0 \leq \psi_{in} \leq \frac{\pi}{6}$$

$$k_{(\psi_{in})} = -\frac{1.2}{\pi}\psi_{in} + 0.7 \cdots \frac{\pi}{6} \leq \psi_{in} \leq \frac{\pi}{2} \tag{11}$$

Figure 6 represents an approximate average response curve for nonisotropic energy-dissipating materials.

To determine the angle of loading, ψ_{in}, for a general pad, consider the vector diagram shown in Fig. 7.

The angle ψ_{in}, between the unit normal to the crushing surface $\mathbf{s}$, and the unit pad fiber vector $\mathbf{g}_{in}$, (which represents the constant orientation of all fibers in the n^{th} pad of the i^{th} element in the vehicle coordinate system) in the direction of $\mathbf{s}$ can be expressed as

$$\cos \psi_{in} = -\mathbf{s} \cdot \mathbf{g}_{in} \tag{12}$$

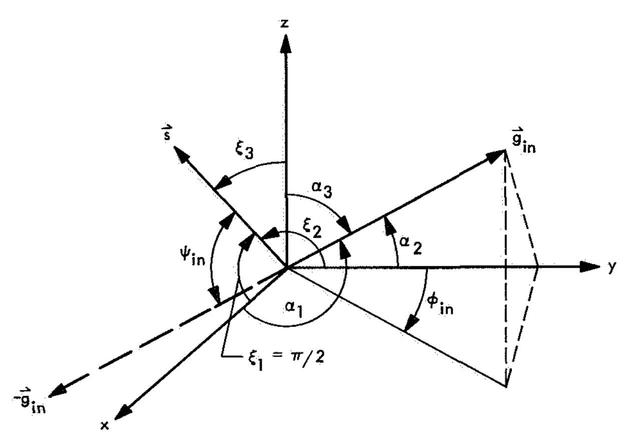

Fig. 7. Vector diagram showing intersection of unit pad fiber and unit surface normal vector

Since the crushing surface is always considered parallel to the x axis

$$\mathbf{s} = \cos \xi_2 \mathbf{j} + \cos \xi_3 \mathbf{k} \qquad (13)$$

where $\mathbf{j}$ and $\mathbf{k}$ are unit vectors along the y and z axes.

But

$$\xi_3 = \xi_2 - \frac{\pi}{2} \qquad (14)$$

and

$$\xi_2 = \frac{\pi}{2} + \theta \qquad (15)$$

Substituting Eqs. (14) and (15) in (13) yields:

$$\mathbf{s} = - \sin \theta \, \mathbf{j} + \cos \theta \, \mathbf{k} \qquad (16)$$

Since a pad fiber can have any spatial orientation

$$\mathbf{g}_{in} = \cos \alpha_1 \, \mathbf{i} + \cos \alpha_2 \, \mathbf{j} + \cos \alpha_3 \, \mathbf{k} \qquad (17)$$

Substituting Eqs. (17) and (18) in (12) gives

$$\cos \psi_{in} = \sin \theta \cos \alpha_2 - \cos \theta \cos \alpha_3 \qquad (18)$$

Recognizing that α_3 remains constant for all pads of a ring element (and therefore must be input in the vehicle description), Eq. (18) may be written, after letting $\alpha_3 = \lambda_i$, as

$$\cos \psi_{in} = \sin \theta \cos \alpha_2 - \cos \theta \cos \lambda_i \qquad (19)$$

where λ_i = angle between $+z$ axis and $\mathbf{g}_{in}$.

Rather than define α_2 for each pad, it is more convenient to define the projection of $\mathbf{g}_{in}$ in the x-y plane. The projection of $\mathbf{g}_{in}$ on the y axis is

$$P_{g_{in}(y)} = \mathbf{g}_{in} \cdot \mathbf{j} = \cos \alpha_2 \qquad (20)$$

The projection of $\mathbf{g}_{in}$ onto the x-y plane is

$$P_{g_{in}(xy)} = |\mathbf{g}_{in}| \cos \left(\frac{\pi}{2} - \lambda_i \right) \qquad (21)$$

Therefore, $P_{g_{in}(xy)} = \sin \lambda_i$

Then from Fig. 7,

$$\cos \phi_{in} = \frac{P_{g_{in}(y)}}{P_{g_{in}(xy)}} \qquad (22)$$

where ϕ_{in} = angle between projection of $\mathbf{g}_{in}$ in x-y plane and $+y$ axis.

Substituting Eqs. (20) and (21) in (22) results in

$$\cos \alpha_2 = \cos \phi_{in} \sin \lambda_i \qquad (23)$$

Then, substituting Eq. (23) in (19) yields

$$\cos \psi_{in} = \sin \theta \sin \lambda_i \cos \phi_{in} - \cos \theta \cos \lambda_i \qquad (24)$$

Since the program assigns numbers to the pads in a consecutive manner in the x-y plane, it is possible to eliminate ϕ_{in} as a user input. Referring to Fig. 3, it is clear that, since the user must provide both β (angle between $+y$ axis and any pad glue line) and N (total number of pads in a limiter element) for every limiter element, the included angle Δ (between two consecutive glue lines in the x-y plane) of any pad may be developed as

$$\Delta = \frac{360}{N} \qquad (25)$$

Then by defining

$$q = \frac{\beta}{\Delta} \qquad (26)$$

the following logic may be applied to this parameter:

If $q = 0$ or an integer, then the value of ϕ_{in} for the n^{th} pad is given by:

$$\phi_{in} = \Delta \left(n - \frac{3}{2} \right) \qquad (27)$$

Substituting Eq. (25) in (27) yields:

$$\phi_{in} = \frac{360}{N} \left(n - \frac{3}{2} \right) \qquad (28)$$

If q = a noninteger

$$\phi_{in} = \Delta \left(n + q_d - \frac{3}{2} \right) \qquad (29)$$

where

$$q_d = \text{decimal portion of } q \qquad (30)$$

Substituting Eq. (25) in (29) yields

$$\phi_{in} = \frac{360}{N} \left(n + q_d - \frac{3}{2} \right) \qquad (31)$$

Solving Eqs. (28) and/or (31) sequentially for each value of n will establish correspondingly fixed values of ϕ_{in} for each pad of the limiter element under consideration.

E. Acceleration of a General Payload Point

Due to angular acceleration effects, it is clear that some points within the payload will experience accelerations greater than that of the vehicle gravity center. The point of maximum acceleration is of interest, since the system design constraint relating to maximum payload acceleration must generally be satisfied for that point.

Furthermore, it is desirable from a design point of view to have the capability to determine accelerations at a discrete point (e.g., a battery gravity center) within the payload as a basis for establishing component design loads. These loads may then be verified through development testing of the prototype vehicle.

For the reasons indicated above, the capability to determine accelerations at four points within the payload has been built into LANDIT. Simply by inputting the vehicle coordinates of the payload points under consideration, the user will receive output describing the total acceleration of each point (at every printout time interval) and both components of the total acceleration vector in the more convenient vehicle coordinate system. The mathematical derivation of the acceleration of a general payload point is presented below.

In vector form (Ref. 8) the acceleration $\mathbf{a}_p$ of a general payload point in the surface coordinate system can be written as:

$$\mathbf{a}_p = \mathbf{a}_G + \dot{\boldsymbol{\theta}} \times (\dot{\boldsymbol{\theta}} \times \mathbf{r}) + \ddot{\boldsymbol{\theta}} \times \mathbf{r} \tag{32}$$

$\mathbf{r}$ = radius vector from vehicle CG to general point p in body-fixed coordinate system.

Also, it is clear that

$$\mathbf{a}_G = \ddot{Y}\,\mathbf{J} + \ddot{Z}\,\mathbf{K} \tag{33}$$

$$\dot{\boldsymbol{\theta}} = \dot{\theta}\,\mathbf{I} \tag{34}$$

$$\ddot{\boldsymbol{\theta}} = \ddot{\theta}\,\mathbf{I} \tag{35}$$

where $\mathbf{I}$, $\mathbf{J}$, and $\mathbf{K}$ = unit vectors along X, Y, Z axes, respectively.

In the vehicle coordinate system, the acceleration vector $\mathbf{a}_G$ of the gravity center and the position vector $\mathbf{r}$ of the general payload point may be written as

$$\mathbf{a}_G = \ddot{y}\,\mathbf{j} + \ddot{z}\,\mathbf{k} \tag{36}$$

$$\mathbf{r} = r_y\,\mathbf{j} + r_z\,\mathbf{k} \tag{37}$$

Pertinent transformation equations between both coordinate systems (Fig. 4) are:

$$\begin{aligned} &\mathbf{J}\cdot\mathbf{j} = \cos\theta \qquad &&\mathbf{K}\cdot\mathbf{j} = -\sin\theta \\ &\mathbf{K}\cdot\mathbf{k} = \cos\theta \qquad &&\mathbf{J}\cdot\mathbf{k} = \sin\theta \\ &\mathbf{I} = \mathbf{i} && \end{aligned} \tag{38}$$

Now to develop $\mathbf{a}_p$ in the vehicle coordinate system it is necessary to determine $\ddot{y}$ and $\ddot{z}$ in terms of $\ddot{Y}$ and $\ddot{Z}$. This is done as follows:

$$\mathbf{a}_G\cdot\mathbf{j} = \ddot{Y}\,\mathbf{J}\cdot\mathbf{j} + \ddot{Z}\,\mathbf{K}\cdot\mathbf{j} = \ddot{y}\,\mathbf{j}\cdot\mathbf{j} + \ddot{z}\,\mathbf{j}\cdot\mathbf{k}$$

Therefore,

$$\ddot{y} = \ddot{Y}\,\mathbf{J}\cdot\mathbf{j} + \ddot{Z}\,\mathbf{K}\cdot\mathbf{j} \tag{39}$$

But through the use of Eq. (38), Eq. (39) becomes

$$\ddot{y} = \ddot{Y}\cos\theta - \ddot{Z}\sin\theta \tag{40}$$

In a similar manner it can be shown that

$$\ddot{z} = \ddot{Y}\sin\theta + \ddot{Z}\cos\theta \tag{41}$$

Substituting Eqs. (40) and (41) in Eq. (36) yields

$$\mathbf{a}_G = (\ddot{Y}\cos\theta - \ddot{Z}\sin\theta)\,\mathbf{j} + (\ddot{Y}\sin\theta + \ddot{Z}\cos\theta)\,\mathbf{k} \tag{42}$$

Through the use of Eq. (38), it can be shown that the relationships for the vector triple product and the vector product of Eq. (32) are, respectively,

$$\dot{\boldsymbol{\theta}} \times (\dot{\boldsymbol{\theta}} \times \mathbf{r}) = -(\dot{\theta})^2\, r_y\,\mathbf{j} - (\dot{\theta})^2\, r_z\,\mathbf{k} \tag{43}$$

$$\ddot{\boldsymbol{\theta}} \times \mathbf{r} = -\ddot{\theta}\, r_z\,\mathbf{j} + \ddot{\theta}\, r_y\,\mathbf{k} \tag{44}$$

Substituting Eqs. (42), (43), and (44) in Eq. (32) yields

$$\mathbf{a}_P = \underbrace{[\ddot{Y}\cos\theta - \ddot{Z}\sin\theta - \ddot{\theta}r_z - (\dot{\theta})^2 r_y]}_{a_{P_y}}\,\mathbf{j} + \underbrace{[\ddot{Y}\sin\theta + \ddot{Z}\cos\theta + \ddot{\theta}r_y - (\dot{\theta})^2 r_z]}_{a_{P_z}}\,\mathbf{k} \quad (45)$$

In Eq. (45), the bracketed coefficients of **j** and **k** represent, respectively, the components of acceleration of the general point P in the y and z directions. The total magnitude of the acceleration of P may be obtained from the relation:

$$a_P = \left[(a_{P_y})^2 + (a_{P_z})^2\right]^{1/2} \quad (46)$$

F. Vehicle Properties

Since the vehicle element geometry must be input to the program, it was desirable to develop and build into LANDIT a set of general relations for determining the vehicle weight, gravity center, and mass moment of inertia in terms of the element coordinates. This capability eliminates the need for the user to perform independent calculations to determine these vehicle properties. The relationships developed, however, involve the payload and limiter weight density parameters which must therefore be input by the user. These parameters are considered constant for each payload and limiter element; however, different values of these parameters may be input for the various elements.

1. Total weight. The total vehicle weight is given by the relation

$$W = \sum_{i=1}^{M} (w_{L_i} + w_{P_i}) \quad (47)$$

where

w_{L_i} = weight of i^{th} limiter element

w_{P_i} = weight of i^{th} payload element

The i^{th} vehicle element can be considered to be composed of both the limiter and payload elements separated by a common boundary—always defined by lines 1-4 of the limiter element description (Section II-A-1). Thus, a limiter element description always defines a corresponding payload triangular element, as indicated in Fig. 1.

Considering the limiter element, it can be shown that by (1) subdividing the limiter element into two triangular sections, and (2) applying Pappus' second theorem (Ref. 9) to volume calculations for both triangular sections, and (3) summing the results, that

$$w_{L_i} = \frac{\pi\rho_{L_i}}{3}\{(y_1 + y_2 + y_3)\,|\,(z_3 - z_2)y_1 - (y_3 - y_2)z_1 + (z_2 y_3 - z_3 y_2)\,| + (y_1 + y_3 + y_4)\,|\,(z_3 - z_4)y_1 - (y_3 - y_1)z_1 + (z_4 y_3 - z_3 y_1)\,|\,\} \quad (48)$$

where

ρ_{L_i} = weight density of i^{th} limiter element

Equation (48) is valid both for quadrilateral elements as well as triangular elements described by four points (see Section II-A-1).

In the same manner it can also be shown that

$$w_{P_i} = \frac{\pi\rho_{P_i}}{3}(y_1 + y_4)\,|\,y_4 z_1 - z_4 y_1\,| \quad (49)$$

where

ρ_{P_i} = weight density of i^{th} payload element

Substituting Eqs. (48) and (49) in Eq. (47) will establish the general relation used in the program to determine the total vehicle weight. The weight calculations are based on the original input element coordinates.

2. Gravity center. Considering a general axisymmetric landing vehicle, such as that depicted by Fig. 1, it is evident that without preliminary calculations the position of the vehicle CG along the z axis is not in general known. Since the equations of motion are written about the vehicle CG, it is essential that the CG position be accurately established. An automated routine for determining the vehicle CG location has been built into LANDIT. The user must input the element geometry in an assumed vehicle coordinate system which has an origin that is contained within the payload and along the z axis. The proper adjustment of the CG location along the z axis will be made by the program.

The fundamental equation used to establish the actual vehicle CG location relative to the assumed vehicle coordinate system is

$$z_V = \sum_{i=1}^{M}\left(\frac{w_{L_i}' z_{L_i}' + w_{L_i}'' z_{L_i}'' + w_{P_i} z_{P_i}}{W}\right) \quad (50)$$

where the subscripted terms L' and L'' relate to the two triangular sections comprising the limiter element, and W and w_{p_i} are given by Eqs. (47) and (49), respectively.

It can be shown that the remaining weight terms of Eq. (50) are given by the relations:

$$w_{L'_i} = \frac{\pi \rho_{L_i}}{3} (y_1 + y_3 + y_4) \mid (z_3 - z_4)y_1 - (y_3 - y_4)z_1 + (z_4 y_3 - z_3 y_4) \mid \quad (51)$$

$$w_{L''_i} = \frac{\pi \rho_{L_i}}{3} (y_1 + y_2 + y_3) \mid (z_3 - z_2)y_1 - (y_3 - y_2)z_1 + (z_2 y_3 - z_3 y_2) \mid \quad (52)$$

The z terms describing the position of the gravity center for each triangular element of Eq. (50) are derived from the general relation (for an i, j, k triangle)

$$z_{t_i} = \frac{\pi \rho_{t_i}}{w_{t_i}} \left[\int_{z_k}^{z_i} (y_{jk}^2 - y_{ik}^2) z \, dz + \int_{z_i}^{z_j} (y_{jk}^2 - y_{ij}^2) z \, dz \right] \quad (53)$$

where the subscript t relates to the triangular element under consideration and,

$$y_{ij} = \frac{1}{(z_i - z_j)} [(y_i - y_j)z + y_j z_i - y_i z_j] \quad (54)$$

$$y_{jk} = \frac{1}{(z_j - z_k)} [(y_j - y_k)z + y_k z_j - y_j z_k] \quad (55)$$

$$y_{ki} = \frac{1}{(z_k - z_i)} [(y_k - y_i)z + y_i z_k - y_k z_i] \quad (56)$$

Although not presented here, the logic necessary to use Eq. (53) properly and to handle the various special cases which may exist has been built into LANDIT.

Based on the result of Eq. (50), the origin of the new vehicle coordinate system is shifted along the z axis by changing the z coordinates of all input element points according to the following rules:

If $z_V > 0$, $-z_V$ is added to all z coordinates.

If $z_V < 0$, $+ z_V$ is added to all z coordinates.

If $z_V = 0$, existing z coordinates are used.

3. ***Mass moment of inertia.*** After the actual vehicle CG location is determined and the new element coordinates established, the program then calculates the vehicle mass moment of inertia. The total vehicle mass moment of inertia I about the true gravity center is obtained from the relation:

$$I = \sum_{i=1}^{M} (I_{L'_i} + I_{L''_i} + I_{P_i}) \quad (57)$$

where the three terms involved in the summation represent, respectively, the mass moment of inertia of the two limiter triangular elements and the corresponding payload triangular element of the i^{th} vehicle element. The expression used to develop the mass moment of inertia of each triangular element is derived from the general relation

$$\bar{I}_{t_i} = \frac{\pi \rho_{t_i}}{4} \left\{ \int_{z_k}^{z_i} [(y_{jk}^4 - y_{ki}^4) - 4(y_{jk}^2 - y_{ki}^2)z^2] \, dz + \int_{z_i}^{z_j} [(y_{jk}^4 - y_{ij}^4) - 4(y_{jk}^2 - y_{ij}^2)z^2] \, dz \right\} \quad (58)$$

where y_{ij}, y_{jk}, and y_{ki} are given by Eqs. (54) through (56), respectively, using the revised element coordinates.

Applying Eq. (58), properly subscripted for each triangular element to Eq. (57), results in the general expression used to determine the total vehicle mass moment of inertia. As in the case of Eq. (53), the logic necessary to use Eq. (59) and to handle all special element cases has been built into the program.

G. Program Termination

Assuming no user input errors are made and no limitations are encountered (see Section III-A-3), LANDIT will terminate each case when one of the following two conditions applies:

(1) Velocity normal to the crushing surface is equal to zero.

(2) Payload has been intersected by the crushing surface.

The first condition implies that the impact limiter material and design configuration was sufficient to dissipate the usually more critical component of impact kinetic energy. The second condition implies that bottoming out of the limiter material has occurred.

H. Program Accuracy

Several comments can be made regarding the engineering accuracy of the final solution. The accuracy of a LANDIT run can be adversely affected by such factors as:

(1) Errors in idealization of an impact attenuating vehicle.

(2) Gross errors in input. These may be indicated by obvious errors in output, but all inputs should be carefully hand-checked.

(3) Program or machine errors. Although a relatively large number of cases has been successfully run and good agreement with a check problem has been obtained, it is still possible that the user may experience such errors.

The user can apply the following tests for solution accuracy as the need arises.

(1) Hand-check the program input.

(2) Study the engineering reasonableness of the program output.

(3) Develop an exact or approximate solution by independent means.

(4) Compare the program results with those of different idealizations of the same configuration.

(5) Compare the program results with test results if available.

III. Programming

A. Input Format

Input to the program is provided in the following blocks.

(1) Comment.

(2) Control.

(3) Vehicle description.

(4) Vehicle initial touchdown condition.

(5) Impact surface characteristics.

(6) Auxiliary payload points.

With the exception of alphameric data in the comment card and some of the data in the control card and the first card of the vehicle geometry description, all input data are written in floating-point numbers. Floating-point numbers must be written with a decimal point in accordance with the format statements included below.

1. Comment. The comment data block consists of a single card of alphameric data containing up to 72 characters. This card is basically used to define the problem being solved and to provide a run record for the user. The first column of this card must be left blank.

2. Control. Program operational contraints are defined on the control card in accordance with the following format:

M	W	W_L	ϵ	τ_i	T	θ_{min}	θ_{max}	$\Delta\theta$	t_p	g	N_1	I

(1I3, 2E7.1, 3E6.4, 3E6.2, 1E6.4, 1E7.2, 1I1, 1E10.5)

M = total number of elements in vehicle description

W = maximum total vehicle weight, lb

W_L = maximum total limiter weight, lb

ϵ = solution error criterion to establish convergence of numerical approximations to the solution of the system of differential equations.

τ_i = initial time step for integrator, sec

T = estimated duration of impact event, sec

θ_{min} = minimum touchdown angle, deg

θ_{max} = maximum touchdown angle, deg

$\Delta\theta$ = touchdown angle increment, deg

t_p = solution print out time interval, sec

g = acceleration due to gravity, ft/sec^2

N_1 = output option
0 Print out solution data
1 Print out and plot solution data

I = total vehicle mass moment of inertia

A positive entry for M implies that the structure is symmetric about the x-y plane. Thus, data for only one quadrant will be accepted by LANDIT. The value of the entry is the number of elements per quadrant and the magnitude of M must be in the range: $1 \leq M \leq 20$. A negative entry for M indicates that all elements in the $+y$ half-plane will be given. The absolute value of the entry equals the total number of elements in this half-plane and the magnitude of M must be in the range: $1 \leq M \leq 40$.

The numerical values entered for maximum vehicle weight W and limiter weight W_L represent the weight limitations imposed by the user on the overall lander design. A calculated total vehicle or limiter weight which is greater than the maximum allowable weight will cause problem termination.

The capability to input an estimated duration of the impact event T was provided basically to enable the user to define a limit to the total program running time.

The three inputs relating to the touchdown angle enable the user to run additional problems at different impact attitudes (all other inputs being held constant). LANDIT will first solve the case for $\theta = \theta_{min}$, and then increment θ by an amount $\Delta\theta$ and solve that case and each successive case up to and including $\theta = \theta_{max}$.

If a positive entry for I is given, LANDIT will use this value as the total vehicle mass moment of inertia. If I is assigned a negative value or zero, the program will then compute the proper value of I and use the computed value as required.

3. ***Vehicle description.*** The vehicle description consists of two data cards for each vehicle element. The number of pairs must agree with the first word on the control card. This section should be coded carefully since the program makes no checks for gaps between or overlap of elements.

The first card of each element pair of cards contains data regarding the limiter element and associated pad geometry. The format is as follows:

y_1	z_1	y_2	z_2	y_3	z_3	y_4	z_4	N	β	λ

8E7.3, 1I2, 2E7.3)

$$\left.\begin{array}{l} y_1 \\ z_1 \\ y_2 \\ z_2 \\ y_3 \\ z_3 \\ y_4 \\ z_4 \end{array}\right\} \text{y and z vehicle coordinates (in.) of corners 1 through 4}$$

N = total number of pads for this limiter element ($2 \leq N \leq 36$)

β = angle between $+y$ axis and any glue line, deg. (see Fig. 3)

λ = angle between $+z$ axis and any pad fiber, deg ($0 \leq \lambda \leq 180$)

The second card describes the material properties of the limiter and associated payload element. The format is as follows:

σ_0	ρ_L	ρ_P

(3E12.6)

σ_0 = axial crushing stress of this limiter element, psi

ρ_L = limiter element weight density, lb/ft^3

ρ_P = payload element weight density, lb/ft^3

4. ***Vehicle initial touchdown conditions.*** The touchdown parameters describing the initial vehicle impact condition must be described on a single card with the following format:

V_o	γ	θ	$\dot{\theta}$

(4E12.6)

V_o = magnitude of impact velocity, fps

γ = angle between $+\bar{Z}$ axis and velocity vector, deg

θ = touchdown angle, deg

$\dot{\theta}$ = impact rotational velocity, deg/s

As shown in Fig. 4, the angle γ is measured in the positive sense from the $+\bar{Z}$ axis to the negatively directed velocity vector, $\mathbf{V}_o$. The range of γ is

$$0 \leq \gamma \leq \pi$$

to account for the cases where $\mathbf{V}_o$ is directed down and to the right (for $\gamma > \pi/2$) in the ground coordinate system.

If a positive value of $\theta (0 \leq \theta \leq 360)$ is input by the user, the program will by-pass the θ option on the control card and perform this specified θ case only. For the θ option to apply, the user must input a value of $\theta = -1.0$.

5. Impact surface characteristics. The format for inputting the impact surface parameters on the surface data card is illustrated below.

α	μ_0

(2E12.6)

α = principal surface slope, deg

μ_0 = coefficient of sliding friction

As shown in Fig. 4, the surface slope angle α is the angle between the $+\bar{Y}$ axis and the impact surface.

6. Auxiliary payload points. The final input data card defines the coordinates of the four auxiliary payload points. The format is as follows.

y_1	z_1	y_2	z_2	y_3	z_3	y_4	z_4

(8E8.3)

$$\left.\begin{array}{l} y_1 \\ z_1 \\ y_2 \\ z_2 \\ y_3 \\ z_3 \\ y_4 \\ z_4 \end{array}\right\} \text{y and z vehicle coordinates (in.) of payload points 1 through 4}$$

B. Output Format

An example of the output format, both printed and plotted, is given in the example problem in the following section. The printed output format is divided into the following basic blocks:

(1) Input data.

(2) Impact response of vehicle gravity center.

(3) Impact response of specially selected payload points.

(4) Mechanical response data.

The total computer running time is printed out at the end of each case.

Upon requesting plotted data, the user will obtain plots of all the printed output response parameters as a function of time. Specially printed data on each plot consists of the vehicle initial touchdown conditions, impact surface characteristics, vehicle total weight and vehicle mass moment of inertia.

C. Flow Chart

The basic flow chart for LANDIT is shown in Fig. 8.

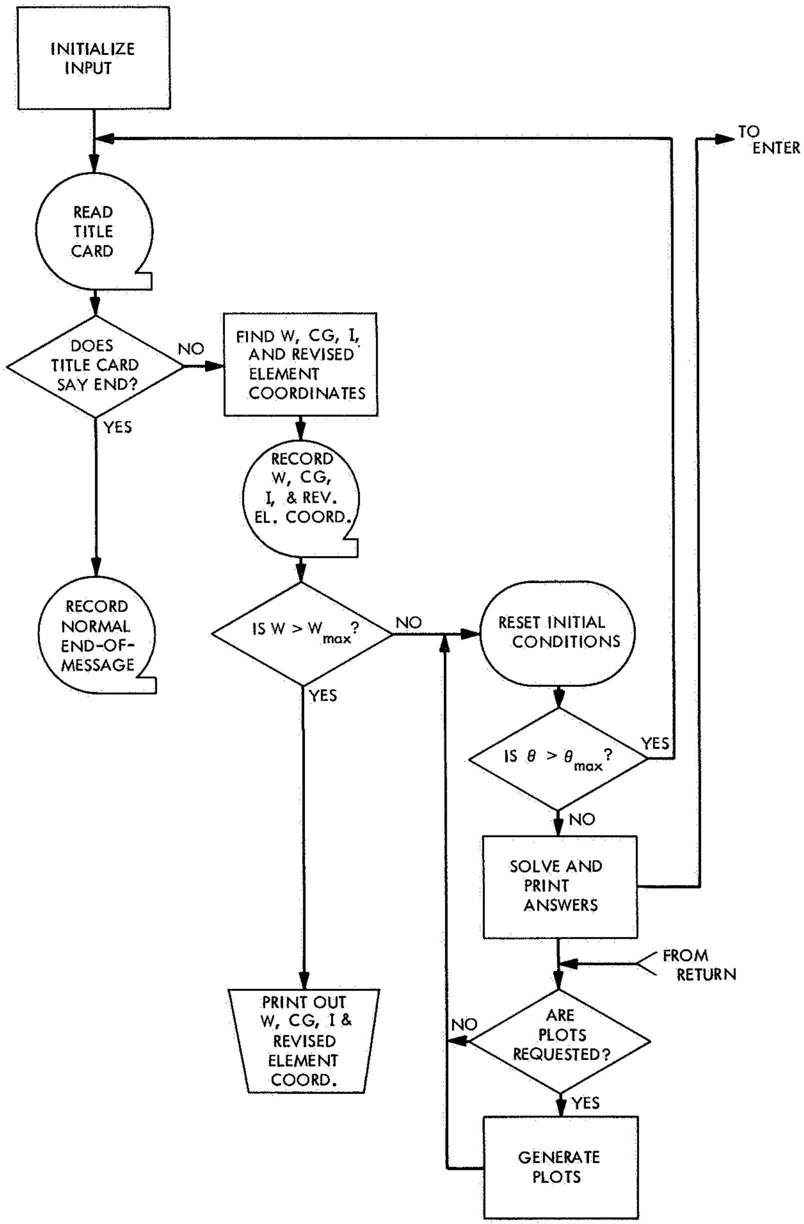

Fig. 8. LANDIT flow chart

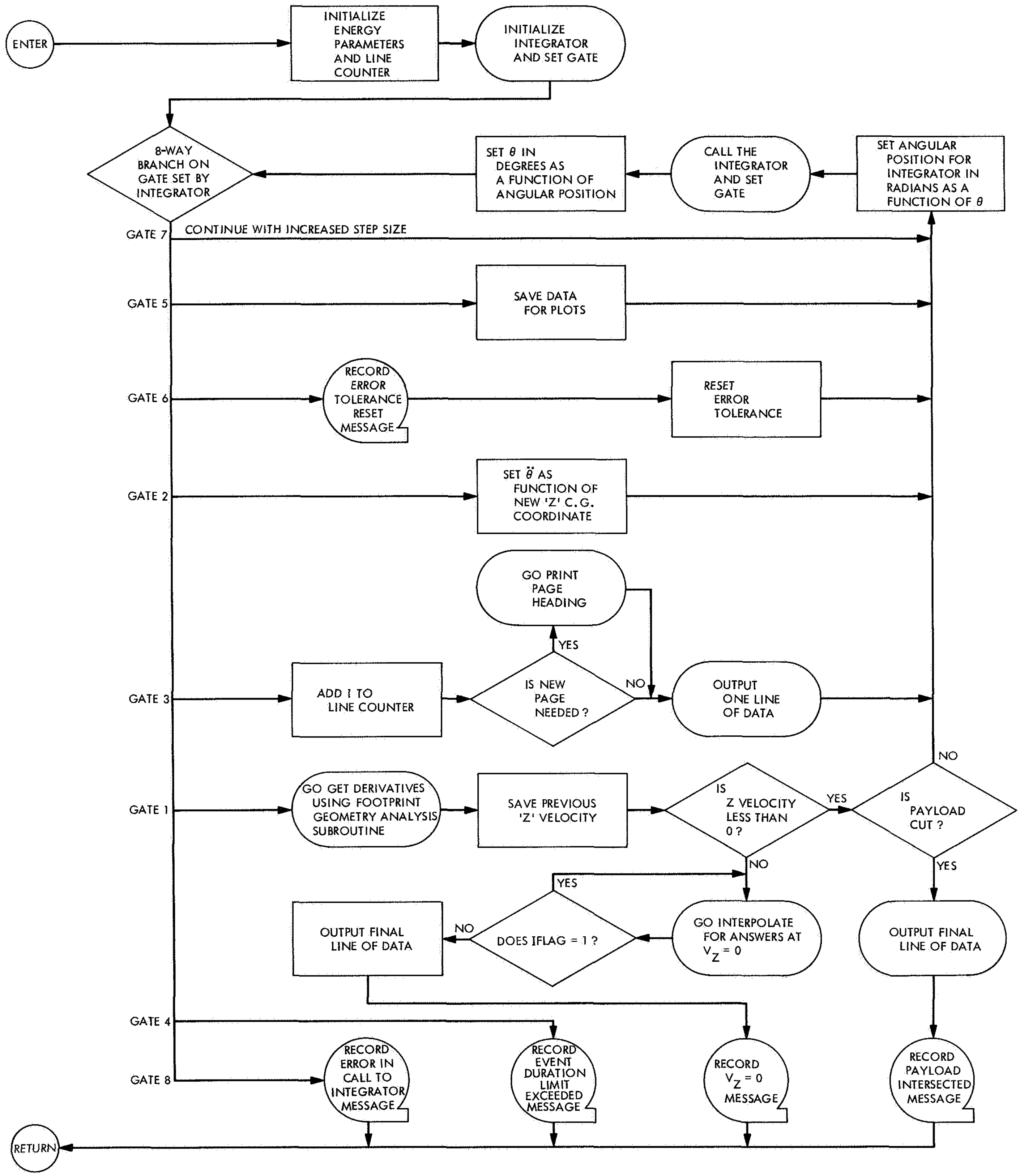
ENTER
INITIALIZE ENERGY PARAMETERS AND LINE COUNTER
INITIALIZE INTEGRATOR AND SET GATE
8-WAY BRANCH ON GATE SET BY INTEGRATOR
SET θ IN DEGREES AS A FUNCTION OF ANGULAR POSITION
CALL THE INTEGRATOR AND SET GATE
SET ANGULAR POSITION FOR INTEGRATOR IN RADIANS AS A FUNCTION OF θ
GATE 7
CONTINUE WITH INCREASED STEP SIZE
GATE 5
SAVE DATA FOR PLOTS
GATE 6
RECORD ERROR TOLERANCE RESET MESSAGE
RESET ERROR TOLERANCE
GATE 2
SET θ̈ AS FUNCTION OF NEW 'Z' C.G. COORDINATE
GO PRINT PAGE HEADING
YES
GATE 3
ADD 1 TO LINE COUNTER
IS NEW PAGE NEEDED ?
NO
OUTPUT ONE LINE OF DATA
NO
GATE 1
GO GET DERIVATIVES USING FOOTPRINT GEOMETRY ANALYSIS SUBROUTINE
SAVE PREVIOUS 'Z' VELOCITY
IS Z VELOCITY LESS THAN 0 ?
YES
IS PAYLOAD CUT ?
NO
YES
YES
OUTPUT FINAL LINE OF DATA
NO
DOES IFLAG = 1 ?
GO INTERPOLATE FOR ANSWERS AT $V_Z = 0$
OUTPUT FINAL LINE OF DATA
GATE 4
GATE 8
RECORD ERROR IN CALL TO INTEGRATOR MESSAGE
RECORD EVENT DURATION LIMIT EXCEEDED MESSAGE
RECORD $V_Z = 0$ MESSAGE
RECORD PAYLOAD INTERSECTED MESSAGE
RETURN

Fig. 8 (contd)

IV. Example Problem

A design sketch of the landing vehicle studied in the example problem is shown in Fig. 9. This disc-type lander was successfully designed, developed and structurally tested under the JPL Capsule System Advanced Development (CSAD) Program conducted during FY 68 (Ref. 10).

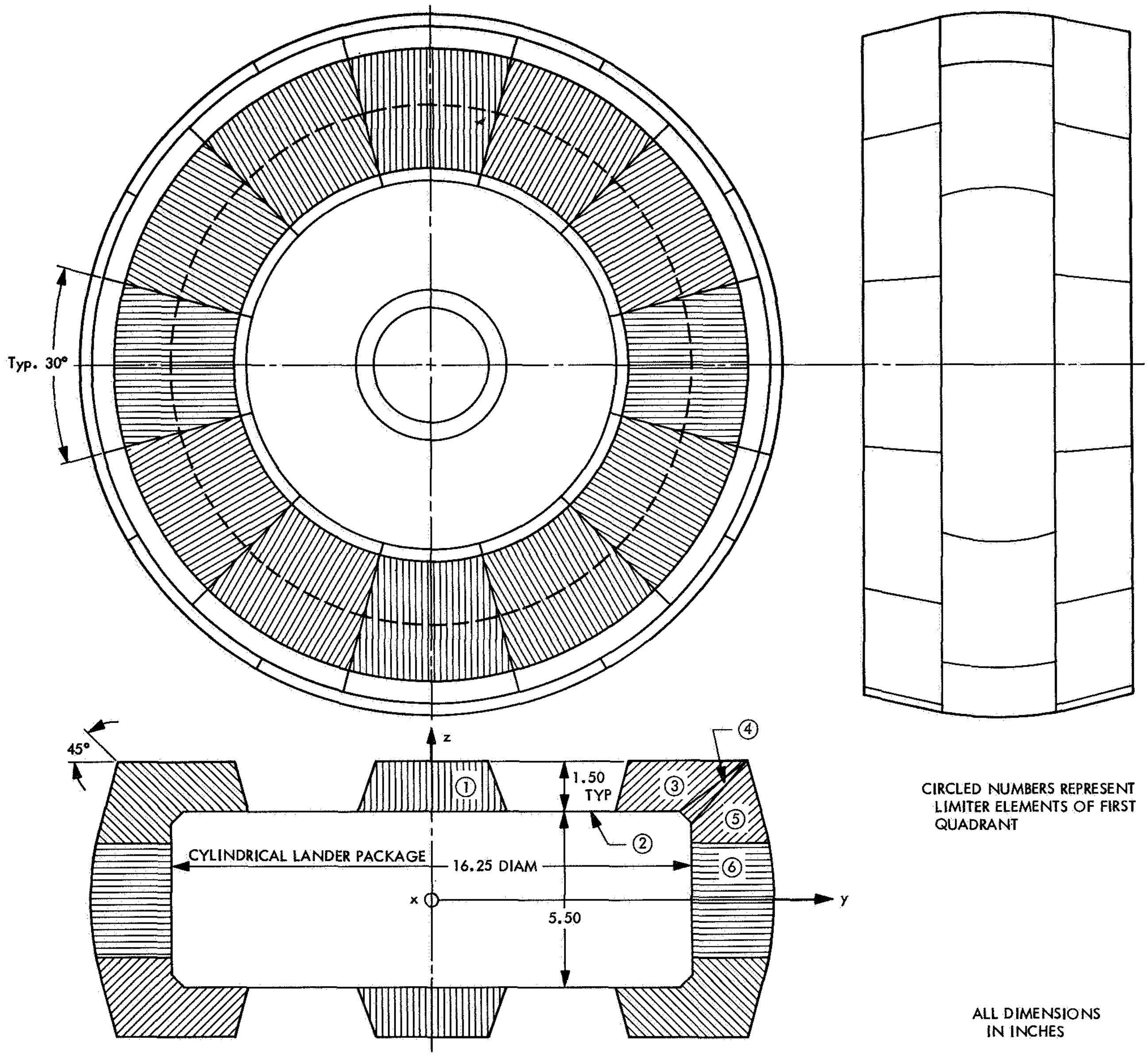

Fig. 9. CSAD impact limiter design sketch

A. Input Data

The following pages are facsimiles of printout input data.

CSAD SLOPE = 20 DEG

INPUT LIMITER ELEMENT COORDINATES (INCHES)

ELEMENT	POINT 1 Y POINT 3 Y	POINT 1 Z POINT 3 Z	POINT 2 Y POINT 4 Y	POINT 2 Z POINT 4 Z
1	0.000000	2.750000	0.000000	4.250000
	1.750000	4.250000	2.250000	2.750000
2	2.250000	2.750000	2.250000	2.750000
	5.625000	2.750000	5.625000	2.750000
3	5.625000	2.750000	6.125000	4.250000
	9.900000	4.250000	7.771400	2.750000
4	7.771400	2.750000	8.835700	3.500000
	9.900000	4.250000	8.125000	2.396400
5	8.125000	2.396400	9.900000	4.250000
	10.727200	1.750000	8.125000	1.750000
6	8.125000	1.750000	10.727200	1.750000
	11.000000	0.000000	8.125000	0.000000
-1	0.000000	-2.750000	0.000000	-4.250000
	1.750000	-4.250000	2.250000	-2.750000
-2	2.250000	-2.750000	2.250000	-2.750000
	5.625000	-2.750000	5.625000	-2.750000
-3	5.625000	-2.750000	6.125000	-4.250000
	9.900000	-4.250000	7.771400	-2.750000
-4	7.771400	-2.750000	8.835700	-3.500000
	9.900000	-4.250000	8.125000	-2.396400
-5	8.125000	-2.396400	9.900000	-4.250000
	10.727200	-1.750000	8.125000	-1.750000
-6	8.125000	-1.750000	10.727200	-1.750000
	11.000000	-0.000000	8.125000	-0.000000

INPUT AUXILIARY PAYLOAD POINT COORDINATES (INCHES)

POINT NUMBER	Y COORDINATE	Z COORDINATE
1	0.0000	0.0000
2	7.7714	2.7500
3	8.1250	2.3964
4	8.1250	0.0000

CSAD SLOPE = 20 DEG

REVISED LIMITER ELEMENT COORDINATES (INCHES)

ELEMENT	POINT 1 Y POINT 3 Y	POINT 1 Z POINT 3 Z	POINT 2 Y POINT 4 Y	POINT 2 Z POINT 4 Z
1	0.000000	2.750000	0.000000	4.250000
	1.750000	4.250000	2.250000	2.750000
2	2.250000	2.750000	2.250000	2.750000
	5.625000	2.750000	5.625000	2.750000
3	5.625000	2.750000	6.125000	4.250000
	9.900000	4.250000	7.771400	2.750000
4	7.771400	2.750000	8.835700	3.500000
	9.900000	4.250000	8.125000	2.396400
5	8.125000	2.396400	9.900000	4.250000
	10.727200	1.750000	8.125000	1.750000
6	8.125000	1.750000	10.727200	1.750000
	11.000000	0.000000	8.125000	0.000000
-1	0.000000	-2.750000	0.000000	-4.250000
	1.750000	-4.250000	2.250000	-2.750000
-2	2.250000	-2.750000	2.250000	-2.750000
	5.625000	-2.750000	5.625000	-2.750000
-3	5.625000	-2.750000	6.125000	-4.250000
	9.900000	-4.250000	7.771400	-2.750000
-4	7.771400	-2.750000	8.835700	-3.500000
	9.900000	-4.250000	8.125000	-2.396400
-5	8.125000	-2.396400	9.900000	-4.250000
	10.727200	-1.750000	8.125000	-1.750000
-6	8.125000	-1.750000	10.727200	-1.750000
	11.000000	-0.000000	8.125000	-0.000000

REVISED AUXILIARY PAYLOAD POINT COORDINATES (INCHES)

POINT NUMBER	Y COORDINATE	Z COORDINATE
1	0.0000	0.0000
2	7.7714	2.7500
3	8.1250	2.3964
4	8.1250	0.0000

CSAD SLOPE = 20 DEG

PAD DESCRIPTION AND MATERIAL PROPERTIES

ELEMENT NO.	NO. OF PADS	GLUE LINE ANGLE (DEG.)	FIBER ANGLE (DEG.)	CRUSHING STRESS (PSI)	LIMITER DENSITY (PCF)	PAYLOAD DENSITY (PCF)
1	4	90.0000	0.0000	1150.00	7.4000	58.0000
2	2	0.0000	0.0000	1150.00	7.4000	58.0000
3	12	105.0000	45.0000	1150.00	7.4000	58.0000
4	12	105.0000	45.0000	1150.00	7.4000	58.0000
5	12	105.0000	45.0000	1150.00	7.4000	58.0000
6	12	60.0000	90.0000	1150.00	7.4000	58.0000
-1	4	90.0000	180.0000	1150.00	7.4000	58.0000
-2	2	0.0000	180.0000	1150.00	7.4000	58.0000
-3	12	105.0000	135.0000	1150.00	7.4000	58.0000
-4	12	105.0000	135.0000	1150.00	7.4000	58.0000
-5	12	105.0000	135.0000	1150.00	7.4000	58.0000
-6	12	60.0000	90.0000	1150.00	7.4000	58.0000

B. Output Data

Facsimiles of printout and plotted output data are presented on the following pages. Only a limited number of plots are shown.

CSAD SLOPE = 20 DEG

CONTROL DATA

THETA RANGE = 10.00	TO	30.00000 DEGS.
THETA INCREMENT	=	15.00000 DEGS.
CONVERGENCE CRITERIA	=	0.10000
INITIAL TIME STEP FOR INTEGRATOR	=	0.00010 SECS.
SOLUTION TIME RANGE = 0 SECONDS	TO	0.10000 SECS.
PRINT OUT TIME INTERVAL	=	0.00020 SECS
TOTAL LANDER WEIGHT LIMITATION	=	50.00000 LBS.
LIMITER WEIGHT LIMITATION	=	10.00000 LBS.

VEHICLE CONSTANTS

MASS MOM. OF INERTIA =	0.2388 SLUG-FT**2
C. G. Z AXIS OFFSET =	0.0000 INCHES
GRAVITY CONSTANT =	32.2000 FT/SEC**2
TOTAL LANDER WEIGHT =	44.7023 LBS.
PAYLOAD TOTAL WEIGHT =	38.0752 LBS.
LIMITER TOTAL WEIGHT =	6.6271 LBS.

SURFACE CONDITION

SLOPE =	20.0000 DEG.
FRICTION COEFF. =	0.6000

VEHICLE C. G. INITIAL CONDITIONS

SURFACE COORDINATE SYSTEM

VERT. DISPLACEMENT(Z) =	8.6295 INCHES
VERT. VELOCITY (DZ) =	-110.2985 FPS
LAT. DISPLACEMENT(Y) =	0.0000 INCHES
LAT. VELOCITY (DY) =	-19.4486 FPS
TOUCH. ANGLE (THETA) =	30.0000 DEG.
ROT. VELOCITY(DTHETA) =	20.0000 DPS

GROUND COORDINATE SYSTEM

TOTAL VELOCITY (DV) =	112.0000 FPS
VELOCITY ANGLE(GAMMA) =	170.0000 DEG.

IMPACT RESPONSE HISTORY

DATA FOR CENTER OF GRAVITY OF LANDER IN SURFACE COORDINATE SYSTEM

TIME MILLISEC.	VERTICAL DISPLACE. (INCHES)	VERTICAL POSITION (INCHES)	VERTICAL VELOCITY (FT/SEC)	VERTICAL ACCEL. (G)	LATERAL POSITION (INCHES)	LATERAL VELOCITY (FT/SEC)	LATERAL ACCEL. (G)	ROTATION POSITION (DEGREE)	ROTATION VELOCITY (DEG/SEC)	ROTATION ACCEL. (RAD/SEC**2)	TOTAL ACCEL. (G)
0.0	0.00	8.63	-110.30	-0.9	0.00	-19.45	-0.3	30.00	20.	2.61	1.
0.2	0.26	8.36	-110.14	61.1	-0.05	-19.38	26.5	29.99	65.	9583.82	67.
0.4	0.53	8.10	-109.43	165.0	-0.09	-19.07	71.4	29.96	260.	24997.44	180.
0.6	0.79	7.84	-107.97	289.0	-0.14	-18.44	125.0	29.88	646.	42604.76	315.
0.8	1.05	7.58	-105.69	422.3	-0.18	-17.45	182.6	29.69	1238.	60730.82	460.
0.9	1.15	7.48	-104.44	474.3	-0.20	-16.91	-0.3	29.57	1556.	43687.25	474.
1.1	1.40	7.23	-100.92	614.4	-0.24	-18.42	-266.3	29.23	1822.	25596.84	670.
1.3	1.64	6.99	-96.53	746.7	-0.29	-20.32	-323.5	28.84	2148.	31319.22	814.
1.5	1.86	6.77	-91.32	869.5	-0.34	-22.57	-376.5	28.37	2539.	36816.75	948.
1.7	2.08	6.55	-85.37	974.9	-0.40	-25.15	-422.1	27.82	2990.	41871.19	1062.
1.9	2.27	6.36	-78.87	1035.8	-0.46	-27.96	-448.4	27.17	3491.	45367.03	1129.
2.1	2.45	6.18	-72.08	1072.7	-0.53	-30.91	-464.4	26.42	4026.	47925.23	1169.
2.3	2.62	6.01	-65.09	1095.2	-0.61	-33.93	-474.1	25.56	4588.	50159.88	1193.
2.5	2.77	5.86	-57.99	1107.0	-0.69	-37.00	-479.2	24.58	5175.	52240.03	1206.
2.7	2.90	5.73	-50.85	1109.5	-0.79	-40.09	-480.3	23.49	5785.	54208.56	1209.
2.9	3.01	5.62	-43.72	1100.8	-0.89	-43.18	-476.5	22.27	6417.	55871.47	1199.
3.1	3.11	5.52	-36.72	1069.4	-0.99	-46.21	-462.9	20.92	7060.	56023.53	1165.
3.3	3.19	5.44	-29.99	1017.3	-1.11	-49.12	-440.4	19.44	7696.	54791.34	1109.
3.5	3.25	5.38	-23.63	956.7	-1.23	-51.88	-414.2	17.84	8314.	53168.94	1043.
3.7	3.30	5.33	-17.69	887.0	-1.36	-54.45	-384.1	16.12	8913.	51224.38	967.
3.9	3.34	5.29	-12.24	801.9	-1.49	-56.81	-347.3	14.28	9486.	48727.74	874.
4.1	3.36	5.27	-7.40	698.1	-1.63	-58.91	-302.4	12.33	10028.	45523.12	761.
4.3	3.37	5.26	-3.36	542.2	-1.77	-60.66	-235.1	10.27	10519.	39180.82	591.
4.5	3.38	5.25	0.00	84.4	-2.00	-62.12	-37.2	6.73	11006.	9408.78	92.

CASE FINISHED ACCOUNT Z VELOCITY = ZERO

CSAD SLOPE = 20 DEG

CONTROL DATA

THETA RANGE = 10.00	TO	30.00000 DEGS.
THETA INCREMENT	=	15.00000 DEGS.
CONVERGENCE CRITERIA	=	0.10000
INITIAL TIME STEP FOR INTEGRATOR	=	0.00010 SECS.
SOLUTION TIME RANGE = 0 SECONDS	TO	0.10000 SECS.
PRINT OUT TIME INTERVAL	=	0.00020 SECS
TOTAL LANDER WEIGHT LIMITATION	=	50.00000 LBS.
LIMITER WEIGHT LIMITATION	=	10.00000 LBS.

VEHICLE CONSTANTS		SURFACE CONDITION		VEHICLE C. G. INITIAL CONDITIONS	
				SURFACE COORDINATE SYSTEM	
MASS MOM. OF INERTIA =	0.2388 SLUG-FT**2	SLOPE =	20.0000 DEG.	VERT. DISPLACEMENT(Z) =	8.6295 INCHES
C. G. Z AXIS OFFSET =	0.0000 INCHES	FRICTION COEFF. =	0.6000	VERT. VELOCITY (DZ) =	-110.2985 FPS
GRAVITY CONSTANT =	32.2000 FT/SEC**2			LAT. DISPLACEMENT(Y) =	0.0000 INCHES
TOTAL LANDER WEIGHT =	44.7023 LBS.			LAT. VELOCITY (DY) =	-19.4486 FPS
PAYLOAD TOTAL WEIGHT =	38.0752 LBS.			TOUCH. ANGLE (THETA) =	30.0000 DEG.
LIMITER TOTAL WEIGHT =	6.6271 LBS.			ROT. VELOCITY(DTHETA) =	20.0000 DPS
				GROUND COORDINATE SYSTEM	
				TOTAL VELOCITY (DV) =	112.0000 FPS
				VELOCITY ANGLE(GAMMA) =	170.0000 DEG.

AUXILIARY PAYLOAD POINT DATA IN VEHICLE COORDINATE SYSTEM

	POINT 1			POINT 2			POINT 3			POINT 4		
TIME	VERT. ACCEL. (G.)	LAT. ACCEL. (G.)	TOTAL ACCEL. (G.)	VERT. ACCEL. (G.)	LAT. ACCEL. (G.)	TOTAL ACCEL. (G.)	VERT. ACCEL. (G.)	LAT. ACCEL. (G.)	TOTAL ACCEL. (G.)	VERT. ACCEL. (G.)	LAT. ACCEL. (G.)	TOTAL ACCEL. (G.)
0.00	-1.0	0.2	1.0	-0.9	0.2	0.9	-0.9	0.2	0.9	-0.9	0.2	0.9
0.20	66.1	-7.6	66.5	258.8	-75.8	269.7	267.6	-67.1	275.9	267.6	-7.6	267.7
0.40	178.6	-20.6	179.7	681.2	-198.9	709.6	704.1	-176.0	725.7	704.2	-21.0	704.5
0.60	312.8	-35.6	314.8	1168.8	-341.4	1217.6	1207.9	-302.5	1245.2	1208.7	-38.3	1209.3
0.80	457.2	-50.6	460.0	1675.4	-492.2	1746.2	1731.4	-437.0	1785.7	1734.3	-60.4	1735.3
0.89	412.4	-234.4	474.3	1285.8	-560.1	1402.5	1326.4	-520.8	1425.0	1331.0	-249.9	1354.2
1.09	406.1	-532.5	669.7	913.7	-735.0	1172.6	938.1	-712.5	1178.0	944.4	-553.7	1094.7
1.29	498.1	-643.5	813.8	1118.0	-894.7	1431.9	1147.9	-867.3	1438.8	1156.7	-673.1	1338.2
1.49	586.1	-744.5	947.5	1312.6	-1046.0	1678.4	1348.1	-1014.1	1686.9	1360.3	-785.7	1570.9
1.69	665.3	-828.3	1062.4	1488.0	-1181.1	1899.8	1528.8	-1145.2	1910.2	1545.7	-885.6	1781.4
1.89	716.7	-871.9	1128.7	1602.7	-1269.5	2044.6	1647.6	-1231.4	2056.9	1670.7	-950.0	1921.9
2.09	754.0	-893.2	1168.9	1682.8	-1333.6	2147.1	1731.2	-1294.2	2161.5	1761.8	-997.0	2024.3
2.29	783.5	-900.2	1193.4	1746.7	-1386.2	2229.9	1798.4	-1346.1	2246.4	1838.2	-1035.1	2109.6
2.49	807.3	-896.3	1206.3	1799.9	-1432.2	2300.2	1855.2	-1391.9	2319.3	1905.8	-1067.9	2184.6
2.69	826.2	-882.7	1209.0	1843.9	-1473.5	2360.3	1902.8	-1433.3	2382.2	1966.0	-1097.1	2251.4
2.89	838.1	-858.1	1199.5	1872.6	-1508.0	2404.3	1935.2	-1468.3	2429.2	2013.0	-1121.8	2304.4
3.09	833.6	-814.3	1165.3	1852.3	-1518.4	2395.1	1917.5	-1481.0	2422.8	2011.6	-1133.6	2309.1
3.29	812.7	-754.0	1108.6	1786.3	-1506.8	2336.9	1852.9	-1473.2	2367.2	1964.8	-1133.3	2268.3
3.49	783.8	-687.5	1042.5	1703.2	-1489.4	2262.6	1771.2	-1460.0	2295.4	1901.8	-1130.3	2212.3
3.69	745.5	-615.3	966.6	1603.5	-1466.6	2173.0	1672.5	-1441.8	2208.2	1822.6	-1124.2	2141.4
3.89	691.4	-534.4	873.8	1476.4	-1432.5	2057.1	1546.0	-1413.0	2094.4	1716.0	-1110.8	2044.2
4.09	617.4	-444.5	760.9	1315.0	-1384.6	1909.5	1384.7	-1371.0	1948.5	1574.6	-1088.6	1914.3
4.29	491.6	-328.0	590.9	1039.7	-1284.7	1652.7	1106.4	-1279.7	1691.7	1315.4	-1036.7	1674.9
4.60	79.5	-46.9	92.3	6.1	-855.9	855.9	48.5	-881.0	882.4	277.3	-822.7	868.2

CASE FINISHED ACCOUNT Z VELOCITY = ZERO

CSAD SLOPE = 20 DEG

CONTROL DATA

THETA RANGE = 10.00 TO		30.00000 DEGS.
THETA INCREMENT	=	15.00000 DEGS.
CONVERGENCE CRITERIA	=	0.10000
INITIAL TIME STEP FOR INTEGRATOR	=	0.00010 SECS.
SOLUTION TIME RANGE = 0 SECONDS TO		0.10000 SECS.
PRINT OUT TIME INTERVAL	=	0.00020 SECS
TOTAL LANDER WEIGHT LIMITATION	=	50.00000 LBS.
LIMITER WEIGHT LIMITATION	=	10.00000 LBS.

VEHICLE CONSTANTS

MASS MOM. OF INERTIA	=	0.2388 SLUG-FT**2
C. G. Z AXIS OFFSET	=	0.0000 INCHES
GRAVITY CONSTANT	=	32.2000 FT/SEC**2
TOTAL LANDER WEIGHT	=	44.7023 LBS.
PAYLOAD TOTAL WEIGHT	=	38.0752 LBS.
LIMITER TOTAL WEIGHT	=	6.6271 LBS.

SURFACE CONDITION

SLOPE	=	20.0000 DEG.
FRICTION COEFF.	=	0.6000

VEHICLE C. G. INITIAL CONDITIONS

SURFACE COORDINATE SYSTEM

VERT. DISPLACEMENT(Z)	=	8.6295 INCHES
VERT. VELOCITY (DZ)	=	-110.2985 FPS
LAT. DISPLACEMENT(Y)	=	0.0000 INCHES
LAT. VELOCITY (DY)	=	-19.4486 FPS
TOUCH. ANGLE (THETA)	=	30.0000 DEG.
ROT. VELOCITY(DTHETA)	=	20.0000 DPS

GROUND COORDINATE SYSTEM

TOTAL VELOCITY (DV)	=	112.0000 FPS
VELOCITY ANGLE(GAMMA)	=	170.0000 DEG.

IMPACT MECHANICAL RESPONSE DATA

TIME	CRUSH FORCE (KIPS)	MECHANICAL ENERGY DISSIPATED (FT-LB)	FRICTIONAL ENERGY DISSIPATED (FT-LB)	MINIMUM DISTANCE TO PAYLOAD FROM SURFACE: ELEMENT	CORNER	DISTANCE (INCHES)
0.00	0.00	0.0	0.0	10	1	-2.362
0.20	3.43	37.8	4.0	10	1	-2.098
0.40	8.04	163.9	13.3	10	1	-1.837
0.60	13.43	357.4	28.4	10	1	-1.585
0.80	19.16	745.8	49.1	10	1	-1.345
0.89	21.24	927.9	58.5	10	1	-1.248
1.09	27.75	1431.4	87.8	10	1	-1.034
1.29	35.23	2053.6	128.7	10	1	-0.834
1.49	40.34	2764.0	180.6	10	1	-0.654
1.69	45.33	3521.3	245.4	10	1	-0.495
1.89	46.74	4277.7	319.8	10	1	-0.361
2.09	48.54	4997.0	405.5	10	1	-0.255
2.29	49.09	5666.7	501.0	10	1	-0.177
2.49	49.62	6274.3	606.6	10	1	-0.130
2.69	49.64	6814.4	721.4	10	1	-0.113
2.89	48.97	7280.7	843.7	10	1	-0.129
3.09	46.53	7664.6	968.5	10	1	-0.179
3.29	44.87	7969.2	1096.9	10	1	-0.263
3.49	41.28	8199.9	1222.0	10	1	-0.379
3.69	39.12	8365.7	1346.8	10	1	-0.529
3.89	34.04	8474.9	1460.4	10	1	-0.711
4.09	30.80	8538.2	1567.4	10	1	-0.924
4.29	20.51	8565.4	1641.0	10	1	-1.165
4.60	3.56	8570.2	1661.6	10	1	-1.611

CASE FINISHED ACCOUNT Z VELOCITY = ZERO

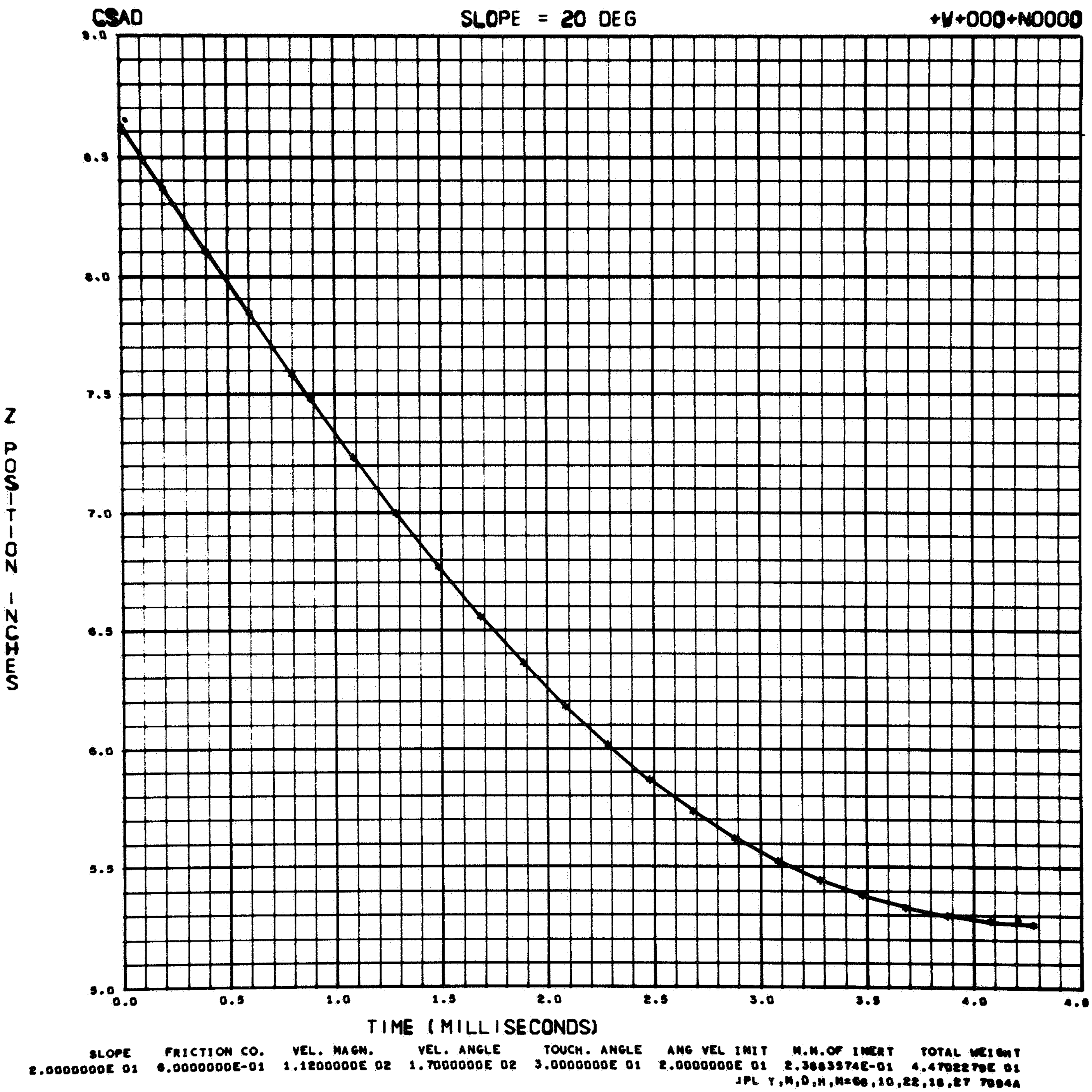
CSAD
SLOPE = 20 DEG
+V+000+N0000
9.0
8.5
8.0
7.5
7.0
6.5
6.0
5.5
5.0
Z POSITION INCHES
0.0
0.5
1.0
1.5
2.0
2.5
3.0
3.5
4.0
4.5
TIME (MILLISECONDS)
SLOPE
FRICTION CO.
VEL. MAGN.
VEL. ANGLE
TOUCH. ANGLE
ANG VEL INIT
M.M.OF INERT
TOTAL WEIGHT
2.0000000E 01
6.0000000E-01
1.1200000E 02
1.7000000E 02
3.0000000E 01
2.0000000E 01

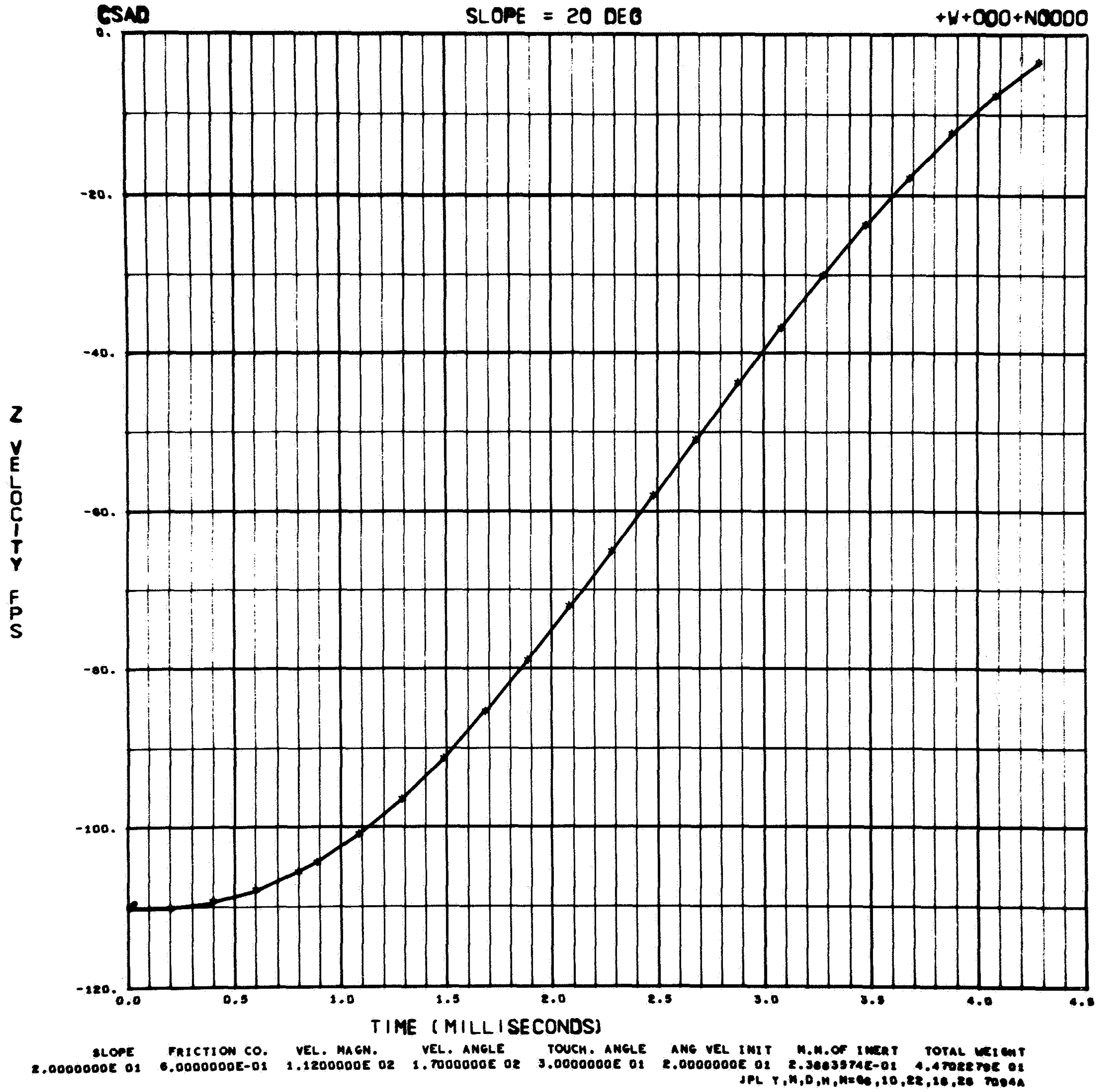
CSAD
SLOPE = 20 DEG
+W+000+N0000
Z VELOCITY FPS
0.
-20.
-40.
-60.
-80.
-100.
-120.
0.0
0.5
1.0
1.5
2.0
2.5
3.0
3.5
4.0
4.5
TIME (MILLISECONDS)
SLOPE FRICTION CO. VEL. MAGN. VEL. ANGLE TOUCH. ANGLE ANG VEL INIT M.M.OF INERT TOTAL WEIGHT
2.0000000E 01 6.0000000E-01 1.1200000E 02 1.7000000E 02 3.0000000E 01 2.0000000E 01 2.3863574E-01 4.4702279E 01
JPL Y,M,D,H,M=66,10,22,16,26 7094A

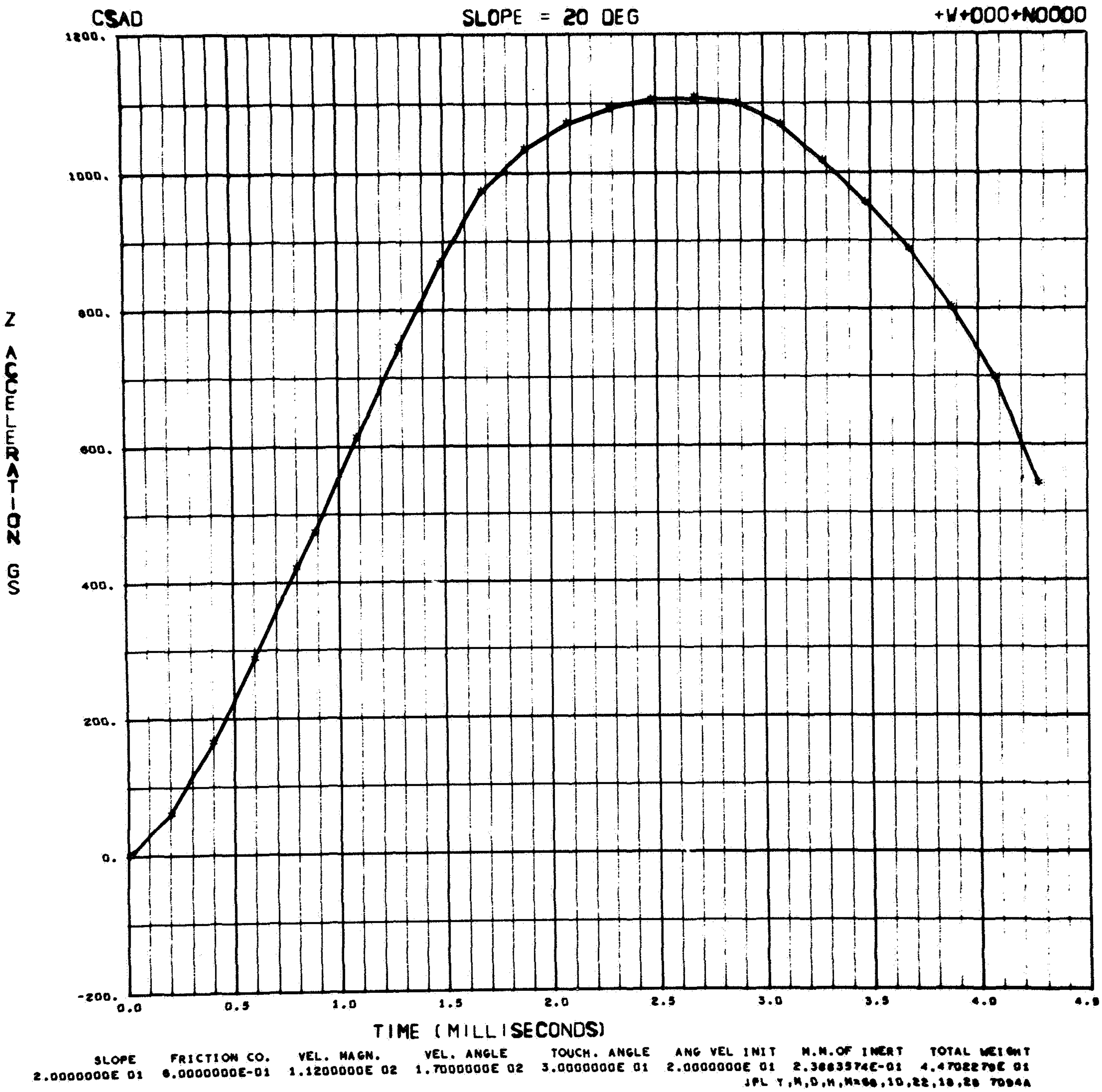

CSAD
SLOPE = 20 DEG
+W+000+N0000
Z ACCELERATION GS
1200.
1000.
800.
600.
400.
200.
0.
-200.
0.0
0.5
1.0
1.5
2.0
2.5
3.0
3.5
4.0
4.5
TIME (MILLISECONDS)
SLOPE 2.0000000E 01
FRICTION CO. 6.0000000E-01
VEL. MAGN. 1.1200000E 02
VEL. ANGLE 1.7000000E 02
TOUCH. ANGLE 3.0000000E 01
ANG VEL INIT 2.0000000E 01
M.M.OF INERT
TOTAL WEIGHT

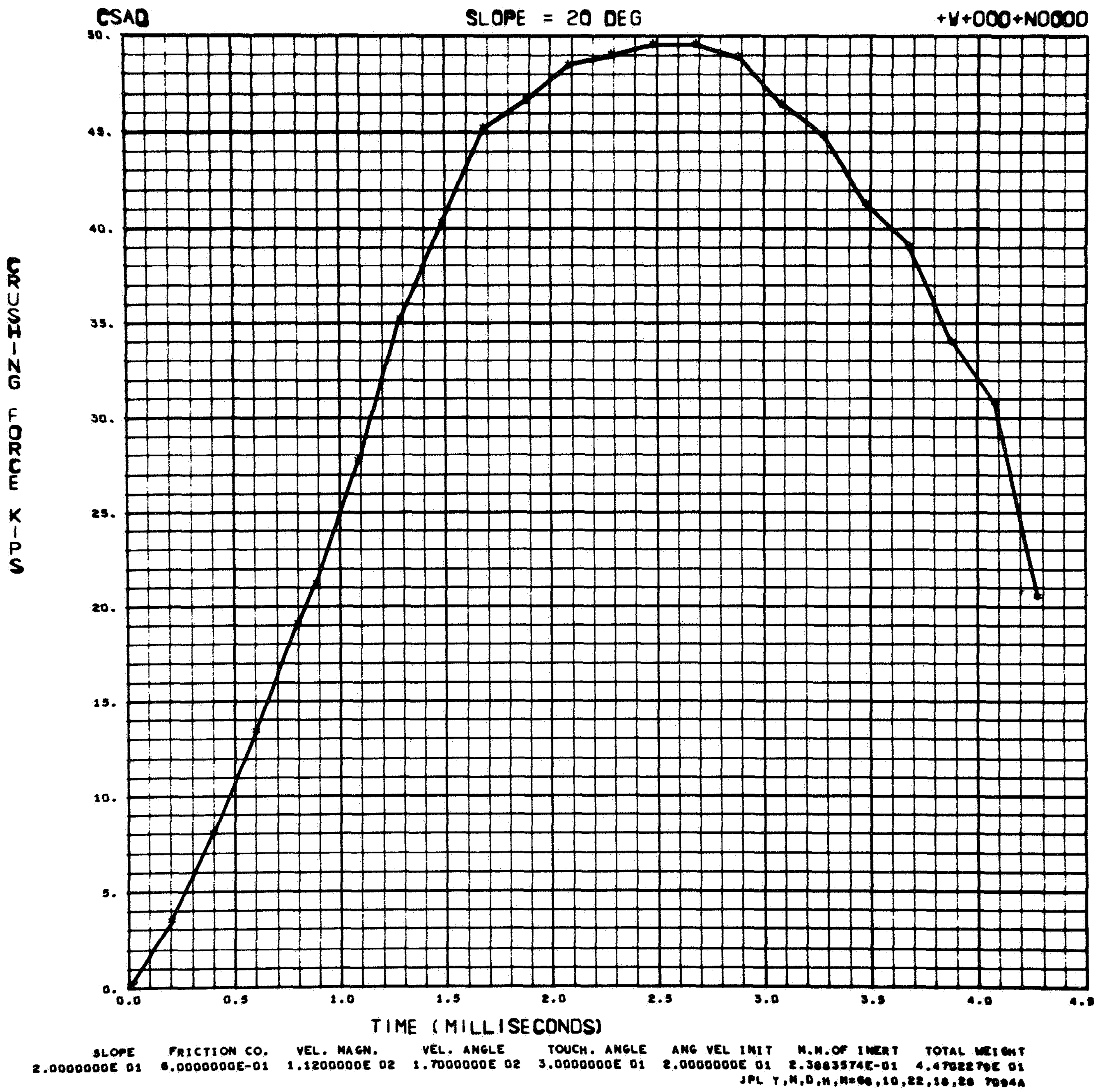
CSAD
SLOPE = 20 DEG
+W+000+N0000
CRUSHING FORCE KIPS
50.
45.
40.
35.
30.
25.
20.
15.
10.
5.
0.
0.0
0.5
1.0
1.5
2.0
2.5
3.0
3.5
4.0
4.5
TIME (MILLISECONDS)
SLOPE FRICTION CO. VEL. MAGN. VEL. ANGLE TOUCH. ANGLE ANG VEL INIT M.M.OF INERT TOTAL WEIGHT
2.0000000E 01 6.0000000E-01 1.1200000E 02 1.7000000E 02 3.0000000E 01 2.0000000E 01

Nomenclature

a acceleration vector

g acceleration due to gravity

$\mathbf{g}_{in}$ unit vector describing fiber orientation of the n^{th} pad of the i^{th} limiter element

i, j, k unit vectors along x, y, z axes

I, J, K unit vectors along X, Y, Z axes

$\bar{I}$ total vehicle mass moment of inertia about actual vehicle CG

$k_{(\psi)}$ off-axis crushing stress reduction parameter

M total number of limiter elements in a vehicle description

N total number of pads in a limiter element

P_Y total instantaneous friction force in Y direction

P_Z total instantaneous crushing force in Z direction

r radius vector from vehicle CG to general point P in body-fixed coordinate system

s unit vector normal to crushing surface

W total vehicle weight

w_i weight of i^{th} element

x, y, z vehicle body-fixed coordinate system

X, Y, Z inertially-fixed surface coordinate system

$\bar{X}, \bar{Y}, \bar{Z}$ inertially-fixed ground coordinate system

$y, \dot{y}, \ddot{y}$ displacement, velocity, acceleration in y direction

$\dot{Y}_A$ moment arm of crushing force

Y_c vehicle velocity at the limiter-surface interface

$Y_G, \dot{Y}_G, \ddot{Y}_G$ displacement, velocity, acceleration of vehicle CG in Y direction

$z, \dot{z}, \ddot{z}$ displacement, velocity, acceleration in z direction

$Z_G, \dot{Z}_G, \ddot{Z}_G$ displacement, velocity, acceleration of vehicle CG in Z direction

α principal surface slope

β angle between $+ y$ axis and any pad glue line

γ angle between impact velocity vector and z axis

Δ pad included angle between two consecutive glue lines in the x-y plane

$\theta, \dot{\theta}, \ddot{\theta}$ angular displacement, velocity, acceleration of vehicle about CG

λ_i angle between $+ z$ axis and $\mathbf{g}_{in}$

μ_o coefficient of sliding friction

ρ_i weight density of i^{th} element

ϕ_{in} angle between projection of g_{in} in X-Y plane and $+ Y$ axis

ψ_{in} angle of loading of the n^{th} pad of the i^{th} limiter element

Subscripts

$(\ )_G$ vehicle CG quantity

$(\ )_L$ impact limiter quantity

$(\ )_P$ payload quantity

$(\ )_V$ vehicle

References

1. *Development of Energy-Dissipating Plastic Honeycomb,* Final Report 68 SD4264, (prepared for JPL under contract 951172). General Electric Company, Space Technology Center, Valley Forge, Pa., June 14, 1968.

2. Knoell, A. C., "Structural Development of an Impact Limiter System for a Mars Landing Vehicle," Paper 68-961, presented at 2nd Aerodynamic Deceleration Systems Conference, El Centro, Calif., Sept. 1968.

3. Garba, J. A., and Bookstein, D., *Surveyor Lunar Touchdown Computer Program: Rigid-Surface Version Usage Document,* Technical Memorandum 33-360. Jet Propulsion Laboratory, Pasadena, Calif., Aug. 15, 1967.

4. Knoell, A. C., *Analysis of the Crushing of a Dovetail Phenolic Honeycomb Spherical Impact Limiter,* Technical Report 32-1287. Jet Propulsion Laboratory, Pasadena, Calif., July 1, 1968.

5. Berkowitz, H. M., and Rodriguez, D. A., "Dynamic Analysis and Development of Response Histories and Trade-off Study Charts for Spherical Impact Limiters," AIAA/ASME paper presented at the 8th Structures, Structural Dynamics and Materials Conference, Palm Springs, Calif., Mar. 29-31, 1967.

6. *RF Transparent, Energy Absorbing, Structural Elements,* Final Report No. 64SD 4329 (prepared for JPL under Contract 950564). General Electric Company, Space Technology Center, Valley Forge, Pa., Aug. 17, 1964.

7. Lenoe, E. M., and Cloutier, G. J., *Impact Attenuating Materials Evaluation Program,* AVCO-RAD Report K420-TR-1, Avco Corp., Wilmington, Mass., Apr. 30, 1965.

8. Housner, G. W., and Hudson, D. E., *Applied Mechanics Dynamics,* 2nd Edition, D. Van Nostrand Company, Inc., Princeton, N. J., Aug. 1959.

9. Singer, F. L., *Engineering Mechanics,* 2nd Edition. Harper & Brothers, New York, N. Y., 1954.

10. Casani, E. K., and Gerpheide, J. H., "System Advanced Development," Paper SD 19, presented at the 19th Congress of the International Astronautical Federation, New York, N. Y., Oct. 1968.